PAPER www.rsc.org/materials | Journal of Materials Chemistry

A novel family of salicylaldimine-based five-ring symmetric and non-symmetric banana-shaped mesogens derived from laterally substituted resorcinol: synthesis and characterization†

Channabasaveshwar V. Yelamaggad,*[a] Manoj Mathews,[a] S. Anitha Nagamani,[a] Doddamane S. Shankar Rao,[a] Subbarao Krishna Prasad,[a] Sonja Findeisen[b] and Wolfgang Weissflog[b]

Received 26th July 2006, Accepted 3rd October 2006
First published as an Advance Article on the web 30th October 2006
DOI: 10.1039/b610758c

We present the results of our extensive investigations into the phase behavior of several ''robust'' five-ring banana-shaped compounds. Six homologous series of either symmetric or non-symmetric bent-core molecules, comprising a laterally substituted 1,3-phenylene ring as the central unit covalently linked to thermally and hydrolytically stable rod-like salicylaldimine segments have been synthesized and evaluated for their mesomorphism. The mesophases have been characterized by optical, calorimetric, X-ray diffraction and electro-optical studies. With a methyl group, polarizable chlorine atom or the more polarizable nitro group as the lateral substituent(s) and terminal alkoxy tails of varying length, the structure–property correlation has been determined. Our study clearly demonstrates that these materials, as predicted, display a different behavior compared to the corresponding compounds without the lateral substituents. The phase behavior shows a critical dependence on the nature and position of the lateral substituent(s). The study includes a comparison with the phase behavior of some of the other types of banana-shaped compounds.

Introduction

Bent-core mesogens, popularly known as banana-shaped liquid crystals (LCs), that are formed by covalently linking two rod-like anisometric segments to a central angular aromatic core represent a distinct and novel class of thermotropic liquid crystals as they form new types of mesophases.[1] Although the earliest report on bent-core molecules goes back to 1929 by Vorlander,[2] the current immense interest in these materials was triggered by investigations of Niori *et al.* in 1996 on a banana-shaped Schiff's base derivative (Chart 1A)[3] synthesized by Matsunaga *et al.*[4] Their study revealed the unique feature of banana-shaped compounds forming electrically switchable polar smectic phases although the constituent mesogens are achiral. Since then numerous bent-core molecules have been synthesized and evidenced to form ferro- and/or antiferro-electric smectic or columnar mesophases and chiral superstructures.[1] The origin of the electrical switching (ferroelectric) behavior in these unique systems is believed to be a consequence of combination of three important factors: (i) the highly polar character of the molecules, (ii) the packing arrangement of the molecules in smectic layers (with the dipoles facing a common direction within the layers) and (iii) the tilt of the molecules in smectic layers with respect to the smectic layer normal.[1,5,6] The different mesophases formed by these compounds are generally termed as ''banana'' (B_n) phases and have been classified into eight categories designated as B_1–B_8 (B stands for bent-core, banana or bow)[1a,7] based on their textural appearance, X-ray diffraction pattern, switching behavior and miscibility studies. In addition, a number of new banana phases have been discovered recently and are not

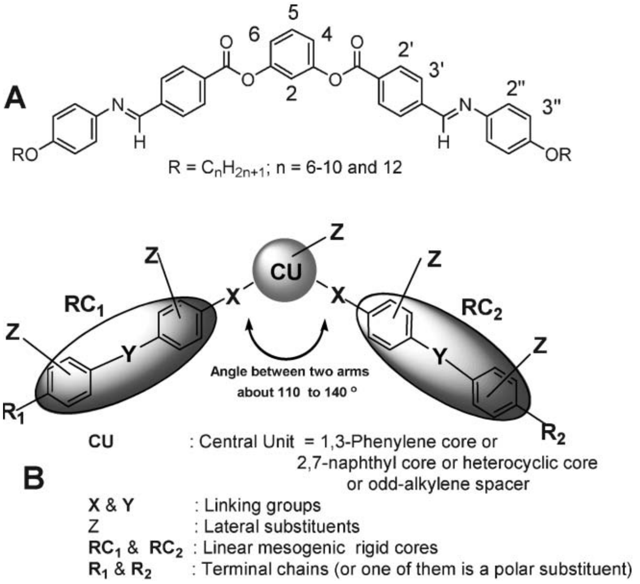

Chart 1 (A) The general molecular structure of the first Schiff's base bent-core compounds shown to exhibit electrical switching behavior, based on which a vast number of similar compounds have been reported; (B) the general template for the molecular structures of banana-shaped mesogens.

---

[a] Centre for Liquid Crystal Research, Jalahalli, Bangalore 560 013, India
[b] Institut für Physikalische Chemie, Martin-Luther-Universität, Halle-Wittenberg, Muhlpforte 1, 06108, Halle (Saale), Germany

† Electronic supplementary information (ESI) available: DSC thermogram; experimental and characterization data. See DOI: 10.1039/b610758c

covered by the nomenclature system mentioned above owing to the fine variations in their mesophase structures. For example, some of the B_n mesophases such as B_1, B_2 and B_7 have several sub-phases with slight structural changes, in which case assigning code letters becomes difficult. Nevertheless, other nomenclature types like SmCP (polar tilted smectic) for B_2, Col_r (rectangular columnar) for B_1 and $SmC_{intercal}$ (intercalated smectic C) for B_6 *etc.* have been used.[1e,7,8] In the present work, both types are adopted for naming the banana fluid phases.

The understanding of the relationship between the chemical structure and LC properties, *viz.*, polarity and chirality of the mesophases formed by banana-shaped materials is not revealed clearly, although a large number of different homologous series of compounds have already been studied.[1] Chart 1B shows a general template that can be used to describe the molecular structure of banana-shaped LCs. From the viewpoint of chemical structure, bent-core molecules with five, six and seven aromatic rings have been found to form LC phases. However, it appears that the existence of banana phases depends not only on the shape of the molecules but also on other parameters such as local dipolar moments and extent of conjugation *etc.*,[1] which in turn depend on various structural fragments like the angular central unit (CU),[1,9–12,] linking groups (X and Y),[13] lateral substituents (Z),[14–17] linear mesogenic rigid cores (RC_1 and RC_2, also called arms or wings)[1,18] and terminal moieties (R_1 and R_2).[5,19–21] Since 1996 a large number of banana-shaped compounds have been synthesized with various combinations of the structural fragments mentioned above. It appears from these synthetic investigations that a minor change in the molecular structure can lead to drastic changes in the mesomorphic behavior and therefore any prediction is extremely difficult. In particular, the introduction of lateral substituent(s) either to the central core or to the inner and outer rings of the banana-shaped compounds is an important structural modification that can alter the thermal behavior. Studies in this direction indicate the dependence of mesomorphic behavior on the position, volume, and electronic (polarizable) properties of the substituents. Specifically, in laterally substituted bent-core compounds the dipolar effects perhaps govern over the steric factors. In most cases, the various substituents in the bent-core molecular fragments induce lower melting and isotropization temperatures. Further, such substitutions either widen the thermal range of the mesophase or destabilize mesomorphism.

Of all the molecular fragments in the bent-core system, the central unit is the key entity as it governs the bending angle (see Chart 1B) between the two rod-like rigid cores attached to it and hence the bent conformation of the molecules. A large number of the banana-shaped LCs reported are five-ring symmetrical Schiff's bases (Chart 1A) derived from resorcinol possessing a 1,3-phenylene core as the central unit connected to two Schiff's base linear mesogenic rigid cores. The structural modifications of these Schiff's bases achieved by introducing various lateral substituents such as fluoro (F), chloro (Cl), cyano (CN), nitro (NO_2) and methyl (CH_3) groups into the central 1,3-phenylene ring at the 2-, 4- and 6-position(s) proved to be very useful for obtaining mesogens with novel phase sequences and lowering the phase transition temperatures.[14] The remarkable thermal behavior of such bent-core compounds, which is attractive from theoretical and fundamental research points of views, truly originates from the position, nature, size and the number of lateral substituents on the central ring. For example, substitution of one chlorine atom into position 4 of the central phenyl ring of the Schiff's base results in materials having rectangular columnar (B_1) and electrically switchable tilted smectic (SmCP) phases with lower transition temperatures compared to their non-substituted analogs.[14c,d] Introduction of one more chlorine atom into position 6 leads to the formation of nematic (N) and smectic C (SmC) mesophases instead of banana phases.[14e] A sequence of switchable SmCP-B_5 phases was obtained for substances having a methyl group in position 2 of the central core[14f] while the corresponding nitro derivatives exhibit the B_7 mesophase.[14g] In such series of compounds having a cyano group in the central ring at position 4, banana phases are seen accompanied by calamitic phases with the phase sequences: isotropic (Iso)–smectic A (SmA)–SmC–SmCP and Iso–N–SmA–SmC–SmCP. Notably, in one of the sequences mentioned above, the SmCP phase occurs below the SmC phase.[14h] Derivatives with groups like cyano, methyl or methoxy at position 5 do not support the formation of mesophases.[14i] Apart from their influence on phase sequences, lateral substitutions can also influence the physical properties of mesophases. The SmCP phase obtained for a Schiff's base derivative with three lateral fluoro substitutions (at position 5 on the central unit and positions 3″ of both terminal rings) shows an unusually high value of spontaneous polarization (P_s) of about 1000 nC cm^{-2}. In contrast, for a compound that has only one fluoro substitution at the central core (at position 5), the P_s is reduced (670 nC cm^{-2}) while the lowest value (370 nC cm^{-2}) was found for a compound with fluoro substitution present only at position 3″.[14a] Thus, introduction of lateral substituents on the Schiff's base banana-shaped compounds significantly influences their LC behavior.

Many of the banana-shaped LCs exhibiting ferroelectric or antiferroelectric mesophases are Schiff's base derivatives showing an unusually broad variety of polymorphism. It is well known that the major drawback of these bent-core compounds is their limited thermal, hydrolytic and photochemical stability owing to the presence of imine linkages. In this direction our group[22] and other research teams have been engaged[23,24] in design, synthesis, and evaluation of mesomorphic properties as well as electro-optic investigations of salicylaldimine-based achiral banana-shaped LCs, which we hereafter refer to as ***BCP-n*** series (Chart 2). The novelty of the molecules originates from the fact that the molecular structure consists of a relatively thermally and hydrolytically stable salicylaldimine unit as a linear rigid segment attached to an angular central 1,3-disubstituted benzene nucleus. The results obtained are quite promising with regard to their stability to heat and moisture owing to the presence of intramolecular hydrogen bonding and stabilization of electrically switchable banana mesophases over a wide thermal range. A systematic investigation focusing on molecular design and synthesis leading to such stable banana-shaped mesogens is very much essential. In particular, lateral substitutions at the central unit of these bent-core molecules would furnish a large number of

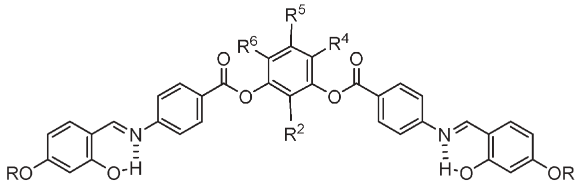

Parent series : **BCP-n** ; R = C_nH_{2n+1}, n = 5-12, 16, 18, 20 and 22

Present series : **BC1-6-n** ; R = C_nH_{2n+1}
Series 1: **BC1-n**; $R^4 = R^5 = R^6 = H$, $R^2 = CH_3$, n = 7 to 12, 16, 18 and 22
Series 2: **BC2-n**; $R^2 = R^4 = R^6 = H$, $R^5 = CH_3$, n = 7 to 12, 16, 18 and 22
Series 3: **BC3-n**; $R^2 = R^5 = R^6 = H$, $R^4 = Cl$, n = 7 to 12, 16, 18 and 22
Series 4: **BC4-n**; $R^2 = R^5 = H$, $R^6 = R^4 = Cl$, n = 7 to 12, 16, 18 and 22
Series 5: **BC5-n**; $R^4 = R^5 = R^6 = H$, $R^2 = NO_2$, n = 8 to 12, 16 and 18
Series 6: **BC6-n**; $R^2 = R^5 = R^6 = H$, $R^4 = NO_2$, n = 6 to 8, 10 to 12, 16 and 18

Chart 2 The general molecular structure of salicylaldimine-based banana-shaped mesogens pertaining to the preceding (**BCP-*n***) and present (**BC1–6-*n***) investigations.

such novel materials that in turn may help in understanding the relation between the molecular structures and thermal behavior, which, to the best of our knowledge, has not been undertaken hitherto. Herein we report the synthesis and characterization of six different series of bent-core compounds, abbreviated as **BC1-*n*** to **BC6-*n*** (see Chart 2), in which the central 1,3-phenylene core is laterally substituted with methyl, nitro or chloro substituents. These substituents, which essentially differ in their steric as well as electronic properties, are expected to exert their influence on the bending angle as well as on the steric packing of the molecules depending on their position on the central unit. The length of the terminal alkoxy tail has been varied to realize several homologues in each series.

Synthesis and molecular structural characterization

The target banana-shaped molecules **BC1-*n*** to **BC6-*n*** series were synthesized as shown in Scheme 1. Derivatives of substituted 1,3-phenylenes (**BC1-*n*** to **BC6-*n*** series) were prepared by reaction of variously substituted resorcinols with two equivalents of the respective 4-(2-hydroxy-4-*n*-alkoxybenzylidineamino)benzoic acids **2a–k** using DCC and a catalytic amount of DMAP in dichloromethane. The required 4-(2-hydroxy-4-*n*-alkoxybenzylideneamino)benzoic acids (**2a–k**) were prepared by acid catalyzed condensation of 4-aminobenzoic acid with 2-hydroxy-4-*n*-alkoxy-benzaldehydes **1a–k** in absolute ethanol. It may be pointed out here these intermediates, **2a–k**, in general, were found to exhibit nematic and/or smectic C phase(s), the details of which are given in the electronic supplementary information (ESI†). The crude materials obtained were recrystallized repeatedly with suitable solvents so that the target compounds obtained were pure and showed a constant isotropic phase transition temperature. Molecular structures of all the target compounds and intermediates were confirmed by spectroscopic methods of analyses (see Experimental part of the ESI† for the details)

General information

The requisite chemicals, namely resorcinols, 2,4-dihydroxybenzaldehyde and 1-*n*-bromoalkanes were obtained from Aldrich company and were used as received. Solvents were purified and dried following standard procedures. The intermediates (**1a–k**) were purified by column chromatography techniques on silica gel (Acme, 60–120 mesh), whereas the acid derivatives (**2a–k**) were purified by repeated recrystallizations using appropriate solvents to constant isotropic phase transition temperature. Thin layer chromatography (TLC) was performed on aluminium sheets pre-coated with silica gel (Merck, Kieselgel10, F254). IR spectra were recorded using a Perkin Elmer Spectrum 1000 FT-IR spectrometer. ^{1}H NMR and ^{13}C NMR spectra were recorded using a Bruker Aveance series DPX-200 (200 MHz) or a BrukerAMX-400 (400 MHz) spectrometer. For ^{1}H NMR spectra, the chemical shifts are reported in ppm relative to tetramethylsilane as an internal standard. Mass spectra were recorded on a Jeol-JMS-600H spectromter in FAB+ mode using 3-nitrobenzyl alcohol as a liquid matrix. Elemental analyses were carried out using a Eurovector EA3000 series CHNOS analyzer. The final compounds as well as acid derivatives were initially evaluated for their LC behavior by the observation of their textural patterns with the help of an optical polarizing microscope (Leitz DMRXP) equipped with a programmable hot stage (Mettler FP90). The transition temperatures and associated enthalpies were obtained from thermograms recorded on a differential scanning calorimeter (Perkin Elmer DSC7) that was calibrated previously using pure indium as a standard. X-Ray diffraction studies of the unoriented samples were carried out using an Image Plate Detector (MAC Science, Japan) equipped with double mirror focusing optics and the sample contained in a Lindemann capillary tube. To examine the electrical switching characteristics of the mesophases, samples in the isotropic phase were placed in the cell (constructed using two indium tin oxide (ITO) coated glass plates pre-treated with a polyimide solution, which enables the molecules to align homogeneously) by capillary action and cooled slowly. Then the electro-optical switching features were observed under the microscope. In order to ascertain the nature (ferro- or antiferro-electric) of the mesophase as well as to determine the P_s, the triangular wave method was followed.

Results and discussion

Four homologous series of symmetrical and two series of non-symmetrical five-ring banana-shaped molecules differing in structure, especially at the central 1,3-phenylene unit, display LC behavior with the exception of two materials. Owing to the presence of lateral substituents like CH_3, NO_2 and Cl at different positions of central unit, these six series of new banana-shaped compounds have been evidenced to exhibit diverse thermal behavior. In particular, the substituents near the linking groups of the central unit enforce changes in the bending angle between the two wings of the bent-core molecules and thus monomorphic to polymorphic behavior has been observed in these six series of compounds. In the following, detailed accounts of the mesomorphic behavior of all the series of mesogens are presented and compared with their parent series and also with other varieties of banana-shaped compounds.[25–34]

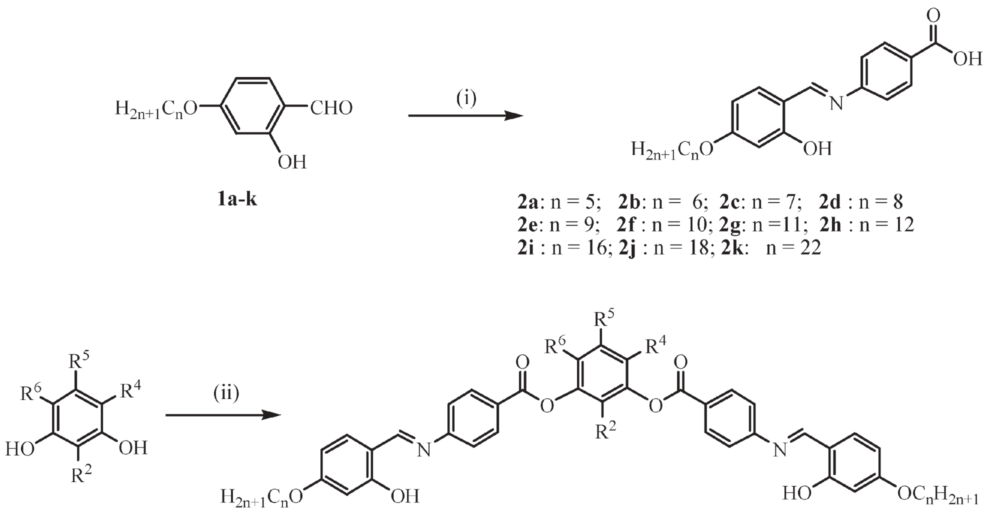

1a-k

2a: n = 5; **2b**: n = 6; **2c**: n = 7; **2d** : n = 8
2e: n = 9; **2f** : n = 10; **2g**: n =11; **2h** : n = 12
2i : n = 16; **2j** : n = 18; **2k**: n = 22

Series 1: **BC1-n :** $R^4 = R^5 = R^6 = H$, $R^2 = CH_3$

BC1- 7 : n = 7; **BC1- 9** : n = 9; **BC1-11**: n = 11 ; **BC1-16**: n = 16; **BC1- 22**: n = 22
BC1- 8 : n = 8; **BC1- 10**: n = 10; **BC1-12**: n = 12 ; **BC1- 18**: n = 18;

Series 2: **BC2-n :** $R^2 = R^4 = R^6 = H$, $R^5 = CH_3$

BC2- 7 : n = 7; **BC2- 9** : n = 9; **BC2-11**: n = 11 ; **BC2-16**: n = 16; **BC2- 22**: n = 22
BC2- 8 : n = 8; **BC2- 10**: n = 10; **BC2-12**: n = 12 ; **BC2- 18**: n = 18

Series 3: **BC3-n :** $R^2 = R^5 = R^6 = H$, $R^4 = Cl$

BC3- 7 : n = 7; **BC3- 9** : n = 9; **BC3-11**: n = 11 ; **BC3-16**: n = 16; **BC3- 22**: n = 22
BC3- 8 : n = 8; **BC3- 10**: n = 10; **BC3-12**: n = 12 ; **BC3- 18**: n = 18

Series 4: **BC4-n :** $R^2 = R^5 = H$, $R^4 = R^6 = Cl$

BC4- 7 : n = 7; **BC4- 9** : n = 9; **BC4-11**: n = 11 ; **BC4-16**: n = 16; **BC4- 22**: n = 22
BC4- 8 : n = 8; **BC4- 10**: n = 10; **BC4-12**: n = 12 ; **BC4- 18**: n = 18;

Series 5: **BC5-n :** $R^4 = R^5 = R^6 = H$, $R^2 = NO_2$

BC5- 8 : n = 8; **BC5- 10**: n = 10; **BC5-12**: n = 12; **BC5-18**: n = 18
BC5- 9 : n = 9; **BC5- 11**: n = 11; **BC5-16**: n = 16

Series 6: **BC6-n :** $R^2 = R^5 = R^6 = H$, $R^4 = NO_2$

BC6- 6 : n = 6; **BC6- 8**: n = 8; **BC6-11**: n = 11; **BC6-16**: n = 16
BC6- 7 : n = 7; **BC6- 10**: n = 10; **BC6-12**: n = 12; **BC6-18**: n = 18

Scheme 1 *Reagents and conditions*: (i) 4-aminobenzoic acid, EtOH, AcOH (catalytic), reflux, 2 h; (ii) **2a–k**, DCC, DMAP, CH_2Cl_2, rt, 48 h.

Thermal behavior of BC1-*n* series

The transition temperatures and the associated enthalpies of **BC1-*n*** series of compounds, in which a methyl group is substituted at position 2 of the 1,3-phenylene core, are summarized in Table 1. All the compounds were found to exhibit monomesomorphic behavior and the enthalpy values obtained in the DSC thermograms for the mesophase to isotropic phase transition were in the range of about 10 to 25 J g^{-1}. On cooling from the isotropic liquid, all the samples, except for the last compound, displayed a mesophase which initially grows as spherulitic domains (Fig. 1a) with a subsequent superposition of a fringe pattern. On further cooling, new layers aggregate outside the initially formed spherulites. If one polarizer is rotated by a small angle (5 to 10 °C) in a clockwise or anticlockwise direction from the crossed position dark domains in the texture become bright and *vice versa* indicating the occurrence of chiral domains with opposite handedness. This texture is quite similar to the ones reported for the SmCP phase.[1] The homologue **BC1-22** exhibits an enantiotropic but different mesophase having the following features. Upon cooling the sample slowly from the isotropic phase, beautiful twisted filaments appear (Fig. 1b) indicating the presence of a helical structure. In the same sample preparation a myelinic texture was also observed. On cooling the sample further, the different textures coalesced into a non-specific pattern. These textural patterns, in particular the occurrence of both single and double wound helices during slow cooling from the isotropic phase, essentially show the features of the two- or three-dimensional antiferroelectric

Table 1 Phase transition temperatures[a] (°C) and corresponding enthalpies [J g^{-1}] of 2-methyl-1,3-phenylenebis[4-(2-hydroxy-4-*n*-alkyloxybenzylidene)-4′-aminobenzoates]: **BC1-*n*** series. Cr = crystal; B_{XA} = two- or three-dimensional antiferroelectric banana (like B_7) mesophase; $SmCP_A$ (B_2) = lamellar antiferoelectric banana mesophase; Iso = isotropic phase. • = Phase exists; — = phase does not exist

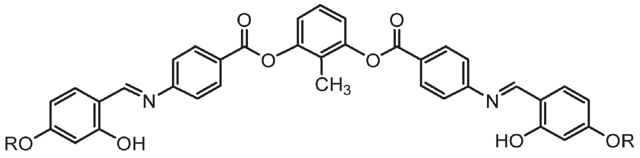

Compound	R	Cr	Heating Cooling	B_{XA}	Heating Cooling	$SmCP_A$	Heating Cooling	I
BC1-7	C_7H_{15}	•	167.4 [17.5] 143.6 [17.8]	—		•	173.8 [19.0] 169.8 [20.5]	•
BC1-8	C_8H_{17}	•	155.5 [11.8][b] 142.4 [11.9]	—		•	173.3 [24.4] 168.8 [18.8]	•
BC1-9	C_9H_{19}	•	152.1 [12.5][b] 144.6 [8.7]	—		•	172.5 [24.1] 167.2 [18.0]	•
BC1-10	$C_{10}H_{21}$	•	151.3 [16.5] 145.3 [13.4]	—		•	174.5 [21.5] 171.7 [22.5]	•
BC1-11	$C_{11}H_{23}$	•	149.3 [15.8][b] 142.3 [13.4]	—		•	171.8 [21.1] 167.6 [16.1]	•
BC1-12	$C_{12}H_{25}$	•	147.7 [16.1][b] 140.5 [14.2]	—		•	171.0 [21.9] 167.7 [18.5]	•
BC1-16	$C_{16}H_{33}$	•	139.7 [62.3] 133.6 [13.7]	—		•	166.1 [19.1] 163.4 [16.2]	•
BC1-18	$C_{18}H_{37}$	•	138.9 [64.3] 130.3 [12.8]	—		•	162.8 [18.4] 160.1 [16.8]	•
BC1-22	$C_{22}H_{45}$	•	135.8 [11.7][b] 127.9 [12.6]	•	153.4 [10.8] 151.1 [10.6]	—		•

[a] Peak temperatures in the DSC thermograms obtained during the first heating and cooling cycles at a rate of 5 °C min^{-1}. [b] Additional crystal to crystal transitions were observed for the compounds **BC1-8** (130.9 [8.2], 147.3 [24.4] and 152.0 [4.1]), **BC1-9** (131.6 [8.7] and 143.2 [27.3]), **BC1-11** (95.6 [4.1]), **BC1-12** (109.3 [7.9]) and **BC1-22** (127.0 [13.4]).

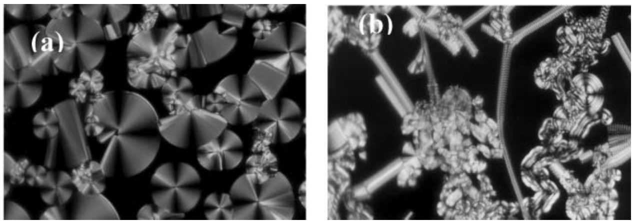

Fig. 1 Photomicrographs of the optical textures observed during cooling just below the isotropic phase for the SmCP (a) and B_{XA} (b) phases of the bent-core molecules **BC1-8** and **BC1-22** respectively.

banana (similar to B_7) phase, and since, as we shall see later, antiferroelectric switching is seen in this sample, we label this phase as B_{XA}.[1,22b]

In order to ascertain the structures of the two different mesophases observed, X-ray diffraction (XRD) experiments were carried out on non-oriented samples. The diffraction patterns were recorded on cooling the sample into the mesophase from the isotropic phase. A representative and typical diffraction pattern obtained for compound **BC1-10** at 165 °C is shown in Fig. 2a (see also Table 2). The diffuse character of the wide angle peak at 4.7 Å indicates a liquid like in-plane order. In the small angle region two sharp reflections were seen with spacings (*d*) 42.9 Å and 21.2 Å. These reflections are in the ratio 1 : 2 indicating a lamellar ordering in the mesophase. The layer spacing is lower than the calculated molecular length of 44.7 Å obtained from the energy minimized conformation with the methylene units in the fully extended form in the all-*trans* conformation,

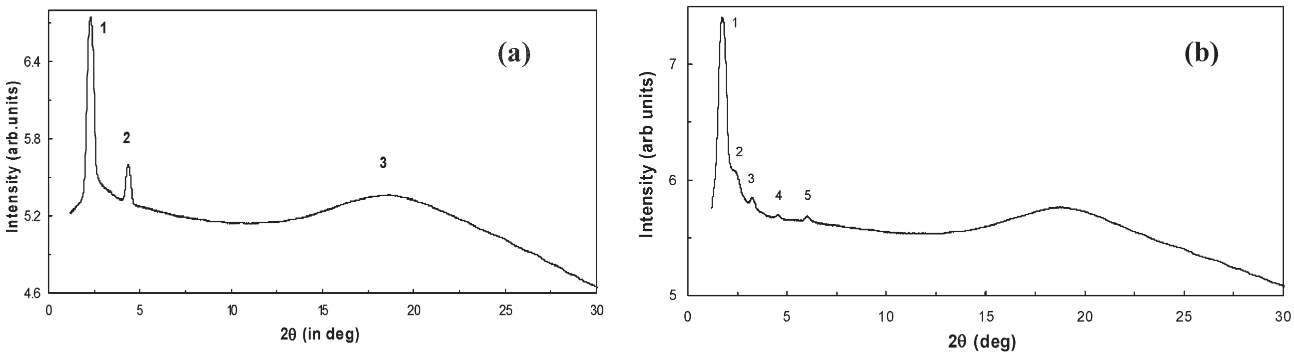

Fig. 2 X-Ray angular intensity profiles obtained in (a) the SmCP phase of **BC1-10** at 165 °C and (b) the B_{XA} phase of **BC1-22** at 145 °C.

Table 2 The spacings (*d*) corresponding to the low angle reflections obtained from XRD studies on different mesophases with the Miller indices (shown in brackets). Also shown are spontaneous polarization (P_s) values obtained in the switchable mesophase. SmA = smectic A phase; SmC = smectic C phase; B_7 = two- or three-dimensional non-switchable mesophase

	Low angle '*d*' values/Å						
Compound (*T*/°C)	d_1	d_2	d_3	d_4	d_5	Mesophase assigned	P_s/nC cm^{-2}
BC1-10 (165)	42.9 (01)	21.2 (02)	—	—	—	$SmCP_A$	436
BC1-22 (145)	59.0	39.9	29.1	20.3	15.1	B_{XA}	404
BC2-12 (145)	43.4 (01)	21.5 (02)	14.3 (03)	—	—	$SmCP_A$	338
BC3-11 (140)	44.9 (01)	21.6 (02)	—	—	—	$SmCP_A$	129
BC3-18 (155)	41.7					SmC	—
BC3-18 (130)	53.2					$SmCP_A$	208
BC3-22 (140)	56.7					SmC	—
BC3-22 (120)	59.9					$SmCP_A$	74
BC5-12 (150)	41.6	20.1	—	—	—	B_7	—
BC5-18 (120)	50.0	—	—	—	—	B_7	—
BC6-7 (112)	39.7 (01)	19.5 (02)	12.8 (03)	—	—	$SmCP_A$	484
BC6-18 (150)	52.7	—				SmA	—
BC6-18 (110)	60 (01)	29.3 (02)				$SmCP_A$	379

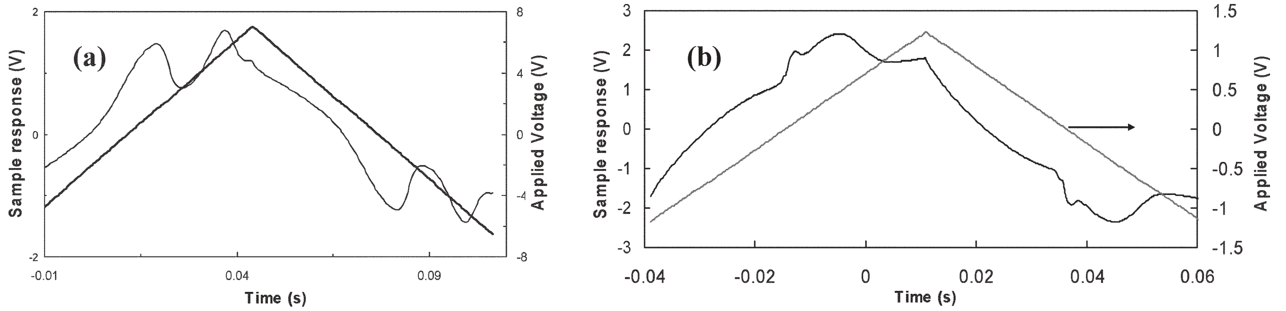

Fig. 3 Electrical switching current response peak obtained by applying a triangular wave field in (a) the SmCP phase of compound **BC1-10** at 155 °C (1.04 V μm^{-1}, 11 Hz) and (b) the B_{XA} phase of compound **BC1-22** at 136 °C (6.4 V μm^{-1}, 10 Hz).

suggesting that this is a tilted smectic phase.[1,22a] On application of a triangular wave electric field (1.04 V μm^{-1}, 11 Hz), the current passing through the sample **BC1-10** showed two peaks per half period of the applied field as shown in Fig. 3a. The two-peak trace shows that the switching observed is of the tri-state antiferroelectric type. These features are commonly observed for the SmCP phase. The combined area under the two peaks is a direct measure of the spontaneous polarization (P_s). The high value of P_s (436 nC cm^{-2}) observed for this sample is typical for the banana-shaped compounds. In view of these observations we assign the phase under discussion as an antiferroelectric SmCP ($SmCP_A$) phase.

The diffraction pattern obtained for the B_{XA} phase of the non-oriented **BC1-22** sample at 145 °C is shown in Fig. 2b. In the wide-angle region, a diffuse peak with spacing (*d*) ~4.7 Å is observed which is indicative of a liquid like order within the smectic layer. In the small angle region five peaks are seen with 59.0 Å, 39.9 Å, 29.1 Å, 20.3 Å and 15.1 Å spacings. These reflections rule out a simple layered phase but point towards a two- or three-dimensional structure. Similar XRD patterns have been reported for the B_7 phases (the exact structural features of which are yet to be ascertained) of other banana-shaped compounds.[1,22b] The electrical switching property of this phase was investigated by the triangular wave method. On application of a triangular wave electric field (6.4 V μm^{-1}, 10 Hz) for the sample **BC1-22** at 136 °C, two peaks per half cycle of the applied field were obtained indicating an antiferroelectric type switching (Fig. 3b). The combined area under the peak is a measure of the P_s and was found to be 404 nC cm^{-2} which is comparable to that reported earlier for the B_7 mesophase of the parent series (**BCP-*n***).[22b] Therefore, it is reasonable to propose that the B_{XA} phase could be a variant (sub-phase) of the novel B_7 mesophase.

It can be seen that in this homologous series of compounds both melting and clearing temperatures decreased with increasing chain length although the mesophase range is not varied. In order to examine the effect of the 2-methyl substitution, the LC behavior of the **BC1-*n*** series of bent-core mesogens was compared with that of the **BCP-*n*** derivatives. Seemingly, in the **BC1-*n*** series the B_7 phase is stabilized only in the case of the compound having a C_{22} chain length, whereas in the parent series of compounds this phase commences from the C_{16} homologue.[22b] In terms of the electrical switching characteristics of both SmCP and B_{XA} phases no significant changes were noticed when compared with the behavior of the **BCP-*n*** series of compounds. Furthermore, the phase behavior of these compounds (**BC1-*n*** series) is comparable to that of the corresponding derivatives in the original banana series:[1a] SmCP phases exist up to high temperatures for most of the homologues. In contrast, reaction of 2-methylresorcinol with 4-(4-*n*-dodecyloxybenzoyloxy)benzoic acid results in a compound containing only ester connecting groups which is not liquid crystalline (mp 121 °C) (unpublished). Inversion of the direction of the outer carboxylic groups results in isomeric

Table 3 Phase transition temperatures[a] (°C) and corresponding enthalpies [J g^{-1}] of 5-methyl-1,3-phenylenebis[4-(2-hydroxy-4-*n*-alkyloxybenzylidene)-4′-aminobenzoates]: **BC2-*n*** series

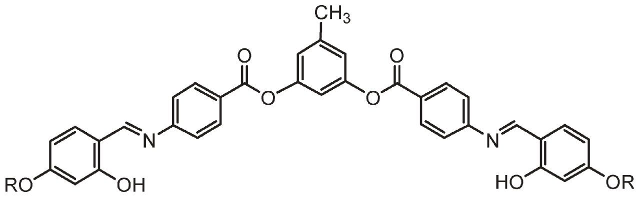

Compound	R	Cr_1	Heating Cooling	Cr_2	Heating Cooling	$SmCP_A$	Heating Cooling	I
BC2-7	C_7H_{15}	•	112.9 [4.6]	•	149.7 [32.2] 143.3 [17.8]	—		•
BC2-8	C_8H_{17}	•	111.5 [5.6]	•	149.1 [30.9] 143.1 [24.3]	—		•
BC2-9	C_9H_{19}	•	146.9 [6.5][b]	•	150.2 [28.1] 143.7 [8.3]	•	— 146.1 [19.3]	•
BC2-10	$C_{10}H_{21}$	•	110.2 [12.2]	•	143.7 [16.2] 140.0 [14.9]	•	152.9 [26.2] 147.6 [20.5]	•
BC2-11	$C_{11}H_{23}$	•	116.2 [17.5]	•	140.4 [14.2] 134.4 [14.3]	•	153.4 [24.0] 148.0 [22.8]	•
BC2-12	$C_{12}H_{25}$	•	117.8 [19.2]	•	136.4 [13.6] 131.3 [13.2]	•	153.2 [22.9] 148.9 [22.4]	•
BC2-16	$C_{16}H_{33}$	•	126.2 [47.8] 120.3 [51.3]	—		•	151.0 [22.7] 145.7 [21.8]	•
BC2-18	$C_{18}H_{37}$	•	126.0 [50.6] 118.1 [52.1]	—		•	148.5 [20.2] 142.9 [16.3]	•
BC2-22	$C_{22}H_{45}$	•	130.3 [54.0] 123.3 [60.7]	—		•	143.3 [14.3] 138.5 [14.1]	•

[a] Peak temperatures in the DSC thermograms obtained during the first heating and cooing cycles at a rate of 5 °C min^{-1}. [b] An additional crystal to crystal transition has been observed for this compound (108.1 [11.1]).

2-methyl-1,3-phenylenebis-4-[4-*n*-alkyloxyphenoxy)benzoates] without liquid crystalline behaviour. As recently published, a crystalline modification is a polar switchable one, which is of high interest.[26,29]

Thermal behavior of BC2-*n* series

It is reported that methyl substitution at position 5 of the central 1,3-phenylene ring is unfavorable for the stabilization of mesophases in five-ring Schiff's base bent-core compounds.[1a,14i] Remarkably, the present salicylaldimine-based (**BC2-*n***) series of compounds with the same central angular core (5-methylresorcinol) exhibit mesomorphism quite convincingly. As illustrated in Table 3, compounds **BC2-7** and **BC2-8** are non-mesomorphic, all the other higher homologues stabilize a mesophase, monotropic in **BC2-9**, but enantiotropic in the rest of the compounds. From the optical textures as well as other physical measurements, the only mesophase observed in these compounds was characterized as $SmCP_A$ phase. Unlike the SmCP phase of other series of compounds, these **BC2-*n*** bent-core molecules exhibited a remarkable and interesting optical textural pattern. Upon very slow cooling the isotropic liquid, the mesophase appears in the form of straight or undulated filaments, which eventually transform into a helical pattern (Fig. 4a) and also, in some regions, coalesce to a highly non-specific textural pattern. On cooling the isotropic liquid at the usual rate (3 to 5 °C min^{-1}), a schlieren texture along with helical patterns are obtained as shown in Fig. 4b. The schlieren texture contained two- and four-brush disclinations (Fig. 4c). This information in conjunction with the existence of a tilted structure as mentioned below indicates the antiferroelectric ground state structure of the mesophase. In some regions, as shown in Fig. 4d, circular domains with equidistant circular stripes were seen, suggesting the helical periodicity of the mesophase. Undoubtedly, some of these optical textures, especially the

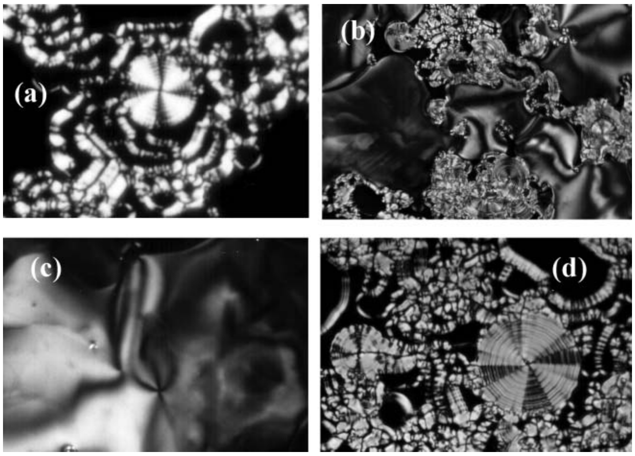

Fig. 4 Microphotographs of the optical textural patterns in different regions of the slide for the SmCP phase of **BC2-12** when cooled from the isotropic phase: (a) straight or undulated filaments, which transform in to a helical pattern; (b) schlieren pattern along with filaments as well as circular domains; (c) schlieren texture having two- and four-brush disclinations; (d) circular domains with equidistant circular stripes developed from the undulated filaments.

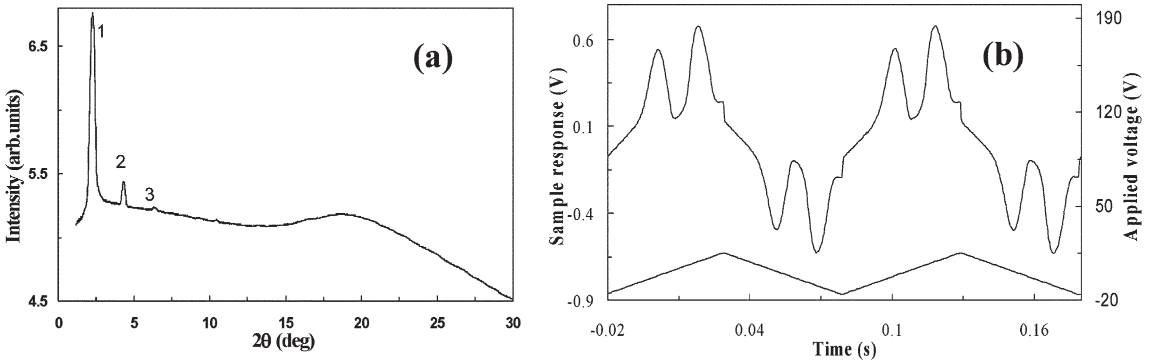

Fig. 5 X-Ray intensity (a) and the current response (b) profiles obtained for the SmCP phase of **BC2-12** at 145 °C and 135 °C respectively.

schlieren defects, are characteristic of the SmCP phase, whereas the occurrence of other patterns suggests it could be a modified version of the SmCP phase.[16e] X-Ray diffraction study was carried out on the SmCP phase of **BC2-12** at 145 °C, as a representative case. In the XRD pattern (Fig. 5a), three reflections in the small angle region with spacings 43.4 Å, 21.5 Å and 14.3 Å are seen which indicate a layered structure. In addition to these reflections a broad diffuse wide-angle reflection at about 4.6 Å shows the absence of in-plane order. The layer spacing is much smaller than the molecular length, *i.e.* l = 56 Å (calculated for the molecule in its all *trans*-conformation) suggesting that this could be a tilted smectic phase. The SmCP phase was investigated for its electrical switching behavior. The current response curve (Fig. 5b) shows two current peaks per half period of an applied triangular wave voltage (3.3 V μm^{-1}, 10 Hz) confirming the antiferroelectric nature of the phase. From the current response, a switching polarization of 338 nC cm^{-2} could be determined.

A dependence of the transition temperatures on the number of carbon atoms in the terminal alkyl chain is clearly evident from Table 3. The clearing temperature, *i.e.* the SmCP phase–isotropic phase transition temperature, rises initially, reaches a maximum and then gradually decreases as the chain length increases. A similar trend is seen for the thermal range of the SmCP phase. However, when compared with the isomeric analogues comprising of 2-methylresorcinol as the central core (**BC1-*n***), the thermal range and P_s value of the SmCP phase seems to have reduced for the **BC2-*n*** banana-shaped compounds. In general, the introduction of a methyl group as a lateral substituent into the central core of five-ring salicylaldimine-based parent molecules (**BCP-*n***) reduces the phase transition temperatures, the thermal range of the mesophases and their ability to form different banana phases.[22] As already mentioned, the attachment of substituents at the top of bent five-ring molecules is disadvantageous for steric reasons: 5-methyl-, 5-cyano- and 5-methoxyresorcinol derivatives do not show mesophases in the original series bearing terminal octyloxy chains.[1a,14i] Therefore, the existence of enantiotropic SmCP phases in the new series **BC2-*n*** is remarkable. Fluorine atoms being the smallest substituents are accepted in the 5 position of five-ring bent-core mesogens.[30,26] Recently, Sadashiva *et al.* reported the mesophase behaviour of five-ring compounds derived from 5-methoxyisophthalic acid.[16a] Larger lateral groups in the 5 position are accepted only if the number of phenyl rings is increased to six or seven and perfluoroalkyl chains exist in the terminal positions.[16e,31]

Thermal behavior of BC3-*n* series

All the nine compounds of the **BC3-*n*** series, possessing chloro substitution at position 4 of the central phenyl ring, exhibit LC behaviour as presented in Table 4. The first homologue **BC3-7** with a heptyloxy terminal chain while cooling from the isotropic phase shows the typical schlieren texture of the nematic phase (Fig. 6) with large director fluctuations. On further cooling, small focal conics with fine stripes across emanate from the nematic phase and finally the field of view fills completely with a focal-conic texture. The N–I transition enthalpy is about 0.5 J g^{-1} whereas it is 6.5 J g^{-1} for the N to the low temperature mesophase transition. The homologues **BC3-8**, **BC3-9**, **BC3-10**, **BC3-11** and **BC3-12** show mono-mesomorphic behaviour and the textural pattern was found to be identical to that of the low temperature phase of **BC3-7**. The striped focal-conic texture observed for **BC3-11** while cooling from the isotropic phase, as a representative case, is shown in Fig. 7a. In a homeotropically aligned sample, schlieren texture is observed, suggesting the optical biaxiality of the phase. In order to ascertain the structure of this biaxial mesophase, an XRD experiment was carried out on a representative sample. The X-ray diffraction pattern obtained at 140 °C for the mesophase of compound **BC3-11** shows a diffuse peak in the wide angle region with d = 4.5 Å that can be attributed to the liquid like in-plane order. In addition, two orders of lamellar reflections at d = 44.9 Å and d = 21.6 Å in the small angle region could be clearly seen. The layer spacing is lower than the theoretical molecular length (l = 55.1 Å) indicating that this could be a tilted smectic phase. The above mentioned textural observations and X-ray diffraction results bear a significant resemblance to the ones observed in the SmCP phase of other banana-shaped compounds.[1,22a]

The characteristic feature of the SmCP phase, namely the electrical switching behaviour was studied using **BC3-11** as a representative compound. The fan-shaped texture with stripes running across the domains (Fig. 7a) obtained by slow cooling, switches above a threshold voltage. Under the polarizing microscope, a textural change was observed (stripes disappear) with a slight increase in birefringence as shown in Fig. 7b. Simultaneously two current peaks could be seen on the oscilloscope screen for the half period of the triangular wave

Table 4 Phase transition temperatures[a] (°C) and the corresponding enthalpies [J g^{-1}] of 4-chloro-1,3-phenylenebis[4-(2-hydroxy-4-*n*-alkyloxybenzylidene)-4-aminobenzoates]: **BC3-*n*** series. N = nematic phase

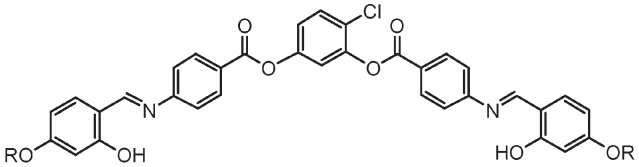

Compound	R	Cr	Heating Cooling	SmCP$_A$	Heating Cooling	SmC	Heating Cooling	SmA	Heating Cooling	N	Heating Cooling	I
BC3-7	C_7H_{15}	•	119.2 [22.8][b] 105.9 [24.0]	•	132.3 [9.8] 129.2 [6.5]	—		—		•	135.1 [0.6] 133.9 [0.5]	•
BC3-8	C_8H_{17}	•	124.9 [17.3] 102.3 [19.8]	•	142.2 [12.1] 138.0 [8.2]	—		—		—		•
BC3-9	C_9H_{19}	•	125.1 [6.8][b] 100.6 [20.1]	•	145.2 [12.1] 143.1 [10.9]	—		—		—		•
BC3-10	$C_{10}H_{21}$	•	117.6 [17.5][b] 94.9 [18.4]	•	145.2 [11.8] 138.9 [7.3]	—		—		—		•
BC3-11	$C_{11}H_{23}$	•	110.5 [78.3] 94.4 [14.6]	•	151.5 [12.3] 146.2 [7.7]	—		—		—		•
BC3-12	$C_{12}H_{25}$	•	104.6 [30.9] 95.0 [15.8]	•	153.0 [12.9] 150.6 [12.1]	—		—		—		•
BC3-16	$C_{16}H_{33}$	•	110.6 [65.6] 92.6 [49.7]	•	150.2 [2.9] 145.1 [2.4]	•	158.8 [7.1] 157.0 [6.3]	—		—		•
BC3-18	$C_{18}H_{37}$	•	111.8 [73.9] 100.4 [65.9]	•	146.3 [2.2] 145.6 [2.2]	•	160.2 [7.0] 159.4 [6.9]	—		—		•
BC3-22	$C_{22}H_{45}$	•	112.9 [76.4] 103.7 [76.5]	•	131.9 [1.3] 129.8 [1.0]	•	153.5 149.0	•	154.7 [3.7][c] 150.7 [3.5]	—		•

[a] Peak temperatures in the DSC thermograms obtained during the heating cycle at a rate of 5 °C min^{-1}. [b] Additional crystal to crystal transitions have been observed for the compounds **BC3-7** (100.4 [48.9]), **BC3-9** (106.2 [17.8], 114.3 [6.6]) and **BC3-10** (77.5 [13.2]). [c] This is the combined enthalpy for the SmC–SmA and SmA–I transitions as the SmC–SmA transition enthalpy could not be obtained due to the existence of the SmA phase for a very short thermal range.

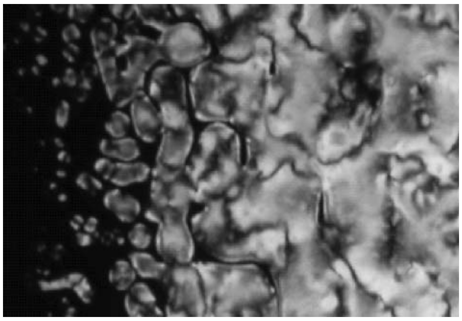

Fig. 6 Photomicrograph of the N phase appearing just below the isotropic phase for compound **BC3-7**.

voltage. The apparent saturated polarization P_s is about 129 nC cm^{-2}. These observations clearly indicate the antiferroelectric nature of this phase. The longer chain length homologues **BC3-16** and **BC3-18** exhibit a dimesomorphic sequence involving a transition from a SmCP to a SmC phase that was evidenced by optical and calorimetric studies. For example, on cooling the sample **BC3-18** from the isotropic phase, the SmC phase exhibits a broken fan-shaped texture for planar alignment and a schlieren texture for homeotropic alignment of the mesogens (Fig. 8a). The textural pattern obtained for the SmCP phase on subsequent cooling is shown in Fig. 8b. The presence of an SmCP phase was confirmed by X-ray diffraction (see Table 2) and electrical switching studies. The tri-state switching yields a P_s value of about 208 nC cm^{-2}. As predicted the SmC phase did not show any response to the applied field.

For the **BC3-22** homologue, the occurrence of three mesophases, *viz.* the SmCP, SmC and SmA phases, was established preliminarily by microscopic and calorimetric studies. The mesophase appearing below the isotropic phase exhibits a focal-conic (Fig. 9a) or a pseudoisotropic texture in

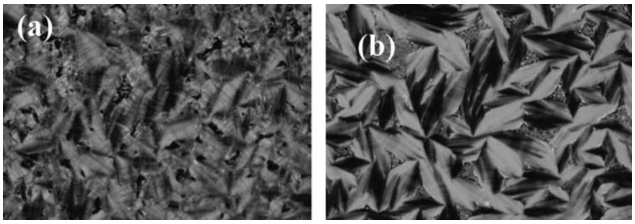

Fig. 7 Photomicrographs of the textures observed for the SmCP phase of **BC3-11** at 136.4 °C: (a) 0 V μm^{-1} and (b) 1.3V μm^{-1}.

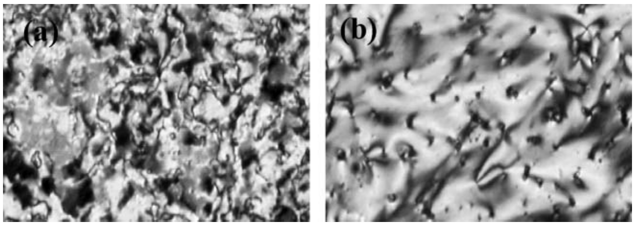

Fig. 8 Photomicrographs of textures observed (a) for the SmC phase at 150 °C and (b) for the SmCP phase at 125.5 °C of **BC3-18**.

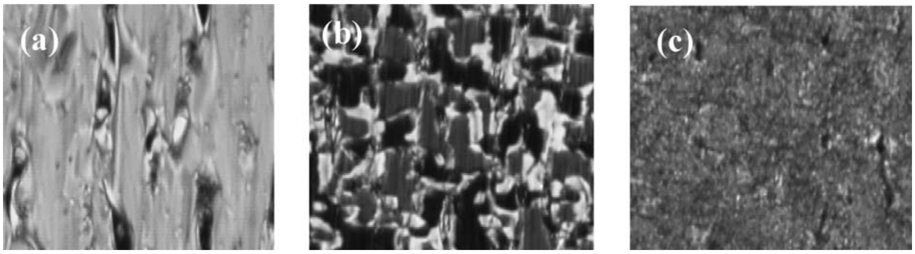

Fig. 9 Photomicrographs of (a) fan-shaped texture of the SmA phase (150 °C), (b) broken fan-shaped texture of the SmC phase (145 °C) and (c) non-specific texture of the SmCP phase (125 °C) observed for **BC3-22**.

slides treated for the planar or homeotropic geometry respectively, which is the characteristic textural behavior of the SmA phase. On cooling, the focal-conic texture is transformed into a broken focal-conic pattern (Fig. 9b), whereas for the homeotropic boundary conditions a schlieren texture is formed indicating the presence of the SmC phase. The SmCP phase occurring below the SmC phase shows a non-specific textural pattern (Fig. 9c) for both planar and homeotropic alignment conditions. The electro-optical investigations performed on these phases showed antiferroelectric switching behavior for the low temperature SmCP phase, while as expected the SmC phase could not be switched. From the current response, a P_s value of about 74 nC cm^{-2} could be determined in the SmCP$_A$ mesophase.

X-Ray measurements (non-oriented samples) indicate a layer structure without in-plane order for all the three mesophases described above. Fig. 10 illustrates the temperature dependence of the layer spacing (*d*) for the SmC and SmCP phases. It should be pointed out here that X-ray studies were not carried out in the SmA phase owing to its short thermal range. As can be seen the layer spacing increases continuously with decreasing temperature at the transition from the SmC to the SmCP phase instead of an expected decrease with decreasing temperature, which is in agreement with the results reported for a similar situation.[14h] It can be assumed that the bent molecules can freely rotate in the SmC phase and at the transition from the SmC to the SmCP phase the long range packing of the molecules in the bent direction becomes more favorable (with tilt of the molecules) for steric reasons. In such a situation for better packing the aliphatic chains stretch out and thereby increasing the layer spacing. The alternating polar direction in subsequent layers causes the antiferroelectric character of the ground state and stabilizes the layer structure of the SmCP phase by minimizing the Coulomb energy.

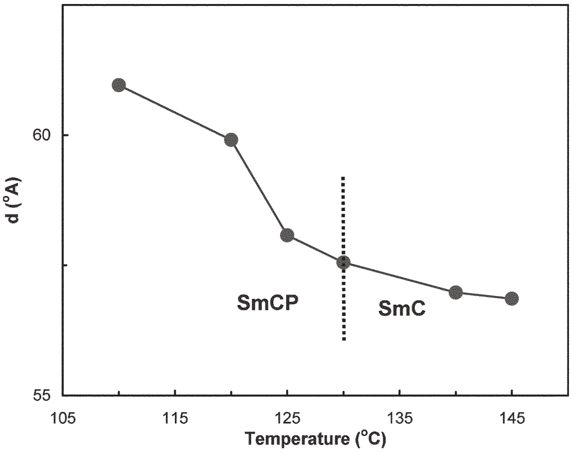

Fig. 10 Temperature dependence of the layer spacing (*d*) in the SmC and SmCP phases of the compound **BC3-22**.

It can be generalized that in these chloro-substituted compounds, the melting as well as clearing temperatures, and thus the mesophase range, are decreased in comparison to the analogous non-substituted derivatives, the parent series of compounds (**BCP-*n***).[22–24] The mesomorphic behavior is also significantly modified; in addition to the SmCP phase characteristic for a bent molecular shape, the SmC and/or the SmA phase occur for the same substance. These observations lead to the conclusion that concerning the chemical constitution, the boundary between calamitic mesogens and banana mesogens is very thin. This is a relatively new aspect concerning the relationships between chemical structure and mesophase behaviour of banana-shaped liquid crystals. Previous NMR investigations suggest that the angle between the two arms of the banana-shaped molecules in the mesophase varies between 105° to 140° depending on the chemical structure of the molecules.[1a,14j] If the angle is greater or smaller than these limits, then calamitic mesophases such as N, SmA or SmC phases occur. In a first approximation, the bending angle is influenced by the chloro atom in position 4 and should be nearly independent of the length of the terminal chains. Such a state can be assumed in the cases of both **BC3-*n*** and **BC6-*n*** (see later for details) series of compounds. Thus, the occurrence of both banana (SmCP) and calamitic (nematic and/or smectic) phases in these bent-core compounds is not surprising. This is in agreement with descriptions not only in the original banana series,[14c,h,j] but also for bent-core mesogens containing ester connecting groups.[33] It may be mentioned here that an unusual polymorphism with a reentrant SmCP phase has been found for derivatives of 4-chlororesorcinol recently.[32] A transition between a polar and a non-polar SmA phase was reported for the corresponding 4-cyanoresorcinol esters.[26,34]

Thermal behavior of BC4-*n* series

In this series of compounds, two chlorine atoms are substituted at positions 4 and 6 of the central 1,3-phenylene ring. The phase transition temperatures and the associated enthalpies obtained for the compounds of the **BC4-*n*** series are summarized in Table 5. Mesophase characterization by optical

Table 5 Phase transition temperatures[a] (°C) and corresponding enthalpies [J g^{-1}] of 4,6-dichloro-1,3-phenylenebis[4-(2-hydroxy-4-*n*-alkyloxybenzylidene)-4′-aminobenzoates]: **BC4-*n*** series

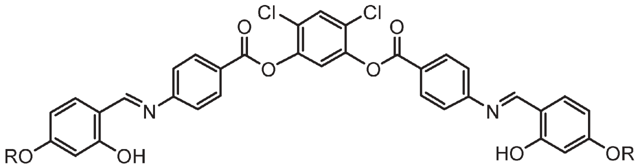

Compound	R	Cr	Heating Cooling	SmC	Heating Cooling	N	Heating Cooling	I
BC4-7	C_7H_{15}	•	133.0 [34.6]	—		•	158.5 [0.8]	•
			94.2 [28.2]				157.3 [0.5]	
BC4-8	C_8H_{17}	•	131.5 [42.8]	—		•	152.2 [1.1]	•
			82.9 [35.3]				149.8 [0.8]	
BC4-9	C_9H_{19}	•	137.2 [35.2]	—		•	159.2 [0.5]	•
			88.4 [20.1]				158.6 [0.4]	
BC4-10	$C_{10}H_{21}$	•	140.2 [44.3]	•	—	•	164.1 [1.4]	•
			99.4 [36.3]		130.5 [0.4]		162.6 [1.3]	
BC4-11	$C_{11}H_{23}$	•	136.5 [49.2]	•	143.9 [0.7]	•	156.2 [1.6]	•
			93.0 [42.4]		139.8 [0.3]		154.2 [1.5]	
BC4-12	$C_{12}H_{25}$	•	135.2 [54.2]	•	155.4 [0.8]	•	159.0 [2.3]	•
			74.8 [16.7]		152.5 [0.4]		158.1 [1.7]	
BC4-16	$C_{16}H_{33}$	•	132.7 [62.9]	•	166.9 [7.3]	—		•
			106.2 [53.2]		165.0 [5.7]			
BC4-18	$C_{18}H_{37}$	•	132.0 [66.1]	•	165.0 [7.6]	—		•
			101.8 [54.4]		162.2 [6.2]			
BC4-22	$C_{22}H_{45}$	•	129.3 [78.1]	•	162.0 [7.3]	—		•
			110.4 [86.5]		160.9 [7.1]			

[a] Peak temperatures in the DSC thermograms obtained during the first heating and cooling cycles at a rate of 5 °C min^{-1}.

textural observation revealed the presence of the N and/or SmC phases. Lower homologues **BC4-7**, **BC4-8** and **BC4-9** stabilized an enantiotropic N phase. Observation of a characteristic texture, in slides treated for planar orientation (unrubbed), namely the schlieren texture having both four- and two-brush defects, evidenced the presence of the N phase. Compound **BC4-10** stabilized a monotropic SmC phase in addition to the enantiotropic N phase. The SmC phase was identified by the observation of a characteristic broken focal-conic texture on glass substrates treated for planar orientation. In compounds **BC4-11** and **BC4-12** both N and SmC phases are enantiotropic in nature. The higher homologues **BC4-16**, **BC4-18** and **BC4-22** displayed only an enantiotropic SmC phase, exhibiting both the broken focal-conic texture and schlieren pattern, when untreated slides were used.

The enthalpies obtained in the range of about 0.5–1.5 J g^{-1} and 6–7 J g^{-1}, respectively, for the N–I and SmC–I phase transitions are in good agreement with values obtained for such phase transitions in calamitic LCs. Not surprisingly, this tilted smectic phase (SmC) was found to be apolar in nature similar to the ones formed by calamitic LCs as evidenced from the lack of any response to the applied electric field. Banana-shaped compounds derived from 1,3-phenylene units with lateral choloro-substitution at the 4 and 6 positions of the central angular ring reported up to now do not form banana mesophases.[1] The introduction of two chlorine atoms into the 4,6 positions of the central core gives rise to a bending angle of about 165° between the two arms favoring the formation of N and/or SmC mesophases. Thus, as anticipated, such behavior was also seen for the compounds **BC4-*n***, a feature in agreement with the behaviour in other series of bent-core compounds.[14e,26,27]

Thermal behavior of BC5-*n* series

The compounds of the series **BC5-*n***, which are substituted with a highly polarizable nitro group at position 2 of the central unit, exhibit identical thermal behavior (Table 6). These bent-core materials, contained between untreated glass slides as thin films, display several fascinating textural patterns appearing concomitantly at different regions. In particular, upon cooling slowly (at a rate of 0.2 °C min^{-1}) from the isotropic phase, elongated single- and double-spiral domains appear. In addition, elongated worms, myelinic texture and two-dimensional patterns were seen. The pitch of the helix seems to be correlated with the cooling rate as previously reported.[1] Under fast cooling (2 °C min^{-1}) rate, thin filaments appearing like threaded beads are formed. When the transition to the liquid crystal phase is completed filaments as well as other patterns collapse to yield a non-specific texture. These patterns are identical to those observed for the mesophase of different series of banana-shaped compounds for which the symbol B_7 has been assigned. Thus, based on microscopic textural observations, the mesophase of the **BC5-*n*** series of compounds is identified as B_7. The wide mesophase range observed during cooling mode for these **BC5-*n*** homologues can be attributed to their tendency to impede the immediate reorganization necessary for crystallization when compared to other series of compounds. For example, compound **BC5-10** did not crystallize while cooling but showed a glass transition at about 70 °C as evidenced by a step like variation in the DSC thermogram. As a representative case the various textural patterns observed

Table 6 Phase transition temperatures[a] (°C) and corresponding enthalpies [J g^{-1}] of 2-nitro-1,3-phenylenebis[4-(2-hydroxy-4-*n*-alkyloxybenzylidene)-4′-aminobenzoates]: **BC5-*n*** series

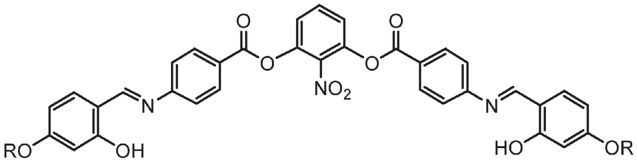

Compound	R	Cr	Heating Cooling	B_7	Heating Cooling	I
BC5-8	C_8H_{17}	•	128.8 [14.0] <40	•	158.8 [23.3] 148.8 [12.0]	•
BC5-9	C_9H_{19}	•	121.3 [17.6] <40	•	150.2 [15.6] 145.0 [13.7]	•
BC5-10	$C_{10}H_{21}$	•	115.9 [10.8][b] 65.4 [0.8][c]	•	168.8 [25.0] 165.2 [18.9]	•
BC5-11	$C_{11}H_{23}$	•	112.3 [12.0][b] 70.4 [2.2][c]	•	156.9 [25.6] 153.2 [20.4]	•
BC5-12	$C_{12}H_{25}$	•	117.0 [20.3] 66.7 [5.4]	•	170.2 [24.1] 163.1 [11.3]	•
BC5-16	$C_{16}H_{33}$	•	113.2 [23.2][b] 85.6 [24.1]	•	163.4 [15.5] 155.7 [7.4]	•
BC5-18	$C_{18}H_{37}$	•	102.3 [64.3] 89.5 [12.8]	•	148.7 [18.7] 143.7 [12.8]	•

[a] Peak temperatures in the DSC thermograms obtained during the first heating and cooling cycle at a rate of 5 °C min^{-1}. [b] Additional crystal to crystal transitions have been observed for the compounds **BC5-10** (64.0 [17.7]) **BC5-11** (74.8 [15.6]) and **BC5-16** (92.9 [28.2]). [c] At this temperature the phase freezes into a glassy state as evidenced by a step like variation in DSC.

for the B_7 phase just below the isotropic phase of compound **BC5-12** are shown in Fig. 11.

In the X-ray pattern of non-oriented samples of **BC5-12** and **BC5-18**, typical diffuse scattering in the wide angle region (d = 4.6 Å) was observed pointing to the liquid like order within the smectic layers. In the small angle region a sharp reflection (at 41.6 Å for **BC5-12** and 50 Å for **BC5-18**) was detected (see Table 2). A similar XRD pattern has been reported recently for the B_7 phase of some of the banana compounds.[13a] Electrical switching studies carried out over a range of temperatures, voltages and frequencies by the application of a triangular wave field did not result in any observable response from the samples. This is not surprising given the fact that the B_7 phase observed for the first time in Schiff's base derivatives[14g] and other banana-shaped compounds with a polar substitution at the 2 position of the 1,3-phenylene derivatives is reported to be non-switchable.[25] Thus, in contrast to the observed current response for the B_{XA} phase of **BC1-22** compound, the B_7 phase shown by this **BC5-*n*** series of bent-core compounds did not show any current response to the applied electric field. This was true not only in our series **BC5-*n***, but also in several series of five-ring bent-core mesogens having different connecting groups.[27,25a,b,28] Thus, attachment of strong polar groups like cyano or nitro between the two legs of the bent molecules is a sure design to prepare materials exhibiting an apolar B_7 phase.

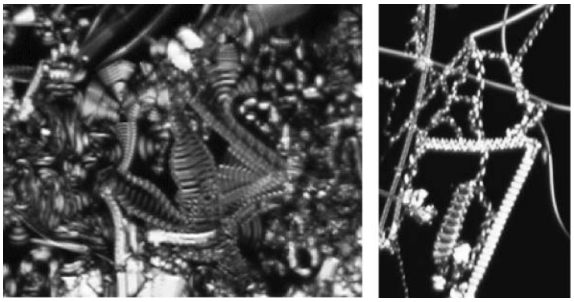

Fig. 11 Optical photographs of the textural patterns of the non-switchable B_7 mesophase obtained for the compound **BC5-12** in different regions of the sample preparation just below the isotropic phase.

Furthermore, the B_7 mesophase observed for the **BC5-*n*** compounds did not show any dependence on the terminal alkyl chain length for its occurrence unlike in the other series of compounds mentioned earlier. Polarizable nitro group substitution at the 2 position not only modifies the type of mesophase formed but also increases the mesophase range in comparison to the analogous 2-methyl derivatives. Further, in the context of the electrical switching behaviour, the B_7 phase formed by these homologues is different from that observed for the higher homologues of the parent series (**BCP-*n***) or that of the B_{XA} phase of the **BC1-22** derivative, *i.e.*, the latter ones show antiferroelectric switching behaviour. Thus the structural features of the B_7 phase seems to be highly complicated and consequently not known yet, although some studies have been initiated in this direction.[1]

Thermal behavior of BC6-*n* series

The **BC6-*n*** series of compounds, to the best of our knowledge, are the first examples of banana-shaped molecules in which a highly polarizable nitro group is substituted at the 4 position of the middle phenyl ring. The transition temperatures and associated enthalpies of this series of compounds are given in Table 7. Phase assignments based on complementary techniques such as optical, DSC, X-ray diffraction and electrical switching studies revealed the presence of two types of mesophases depending on the length of the terminal alkyl chains. As shown in Table 7, for the isotropic mesophase (especially for the banana phase) transition, the enthalpy (ΔH) value obtained for the first cooling cycle is nearly half that in the first heating scan. A similar tendency is also seen for some of the compounds of **BC5-*n*** series as shown in Table 6. However, during the subsequent (second) heating/cooling runs, the ΔH value obtained agrees with that of first cooling (see ESI†) scan with a shift in the phase transition temperature. Currently, we do not have an understanding of this feature.

On cooling from the isotropic liquid, the phase formed by the lower homologues **BC6-6**, **BC6-7**, **BC6-8**, **BC6-10**, **BC6-11** and **BC6-12** emerges as bâtonnets which coalesce to form broken fan shaped textures as shown in Fig. 12a. In different regions of the cell a schlieren texture is also obtained (Fig. 12b). As a representative case, the X-ray angular intensity profile was obtained for a non-oriented sample of **BC6-7** at 112 °C. The diffractogram showed a strong Bragg reflection in the small angle region with two harmonics, suggesting a layer structure. The diffuse scattering maxima in the wide angle region indicated a liquid like order within the layer. The layer

Table 7 Phase transition temperatures[a] (°C) and corresponding enthalpies [J g^{-1}] of 4-nitro-1,3-phenylenebis[4-(2-hydroxy-4-*n*-alkyloxybenzylidene)-4′-aminobenzoates]: **BC6-*n*** series

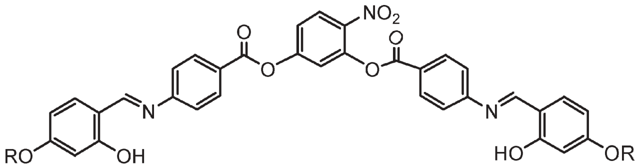

Compound	R	Cr	Heating Cooling	SmCP$_A$	Heating Cooling	SmA	Heating Cooling	I
BC6-6	C_6H_{13}	•	114.5 [17.6] 98.9 [14.1]	•	174.6 [18.9] 161.7 [11.7]	—		•
BC6-7	C_7H_{15}	•	104.9 [10.9][b] 89.9 [7.7]	•	178.8 [15.7] 165.2 [9.1]	—		•
BC6-8	C_8H_{17}	•	97.1 [9.9][b] 80.1 [2.4]	•	181.5 [18.8] 166.7 [7.9]	—		•
BC6-10	$C_{10}H_{21}$	•	90.9 [9.8][b] 70.3 [7.8]	•	176.4 [15.2] 158.1 [7.5]	—		•
BC6-11	$C_{11}H_{23}$	•	92.8 [10.5][b] 68.0 [20.4]	•	184.6 [25.6] 177.7 [15.3]	—		•
BC6-12	$C_{12}H_{25}$	•	94.9 [6.9][b] 64.6 [15.3]	•	182.5 [19.6] 171.3 [7.4]	—		•
BC6-16	$C_{16}H_{33}$	•	107.1 [51.5][b] 68.2 [15.6]	•	161.5 [5.6] 116.8[c]	•	173.6 [5.6] 173.1 [4.2]	•
BC6-18	$C_{18}H_{37}$	•	110.8 [47.7][b] 69.0 [17.7]	•	162.2 [5.9] 111.0[c]	•	172.3 [5.1] 171.3 [4.0]	•

[a] Peak temperatures in the DSC thermograms obtained during the first heating and cooling cycle at a rate of 5 °C min^{-1}. [b] Additional crystal to crystal transitions have been observed for the compounds **BC6-7** (89.1 [16.2]), **BC6-8** (87.4 [20.2]), **BC6-10** (67.5 [52.7]), **BC6-11** (58.7 [11.2], 84.6 [17.9]), **BC6-12** (77.8 [59.2]), **BC6-16** (88.2 [42.6]) and **BC6-18** (95.1 [21.5]). [c] Determined by the textural change observed in POM, and a corresponding enthalpy change was not observed in DSC.

spacing was found to be relatively lower than the calculated molecular length (in its all *trans*-conformation) suggesting that this is a tilted smectic phase. The switching behavior of this phase was investigated by applying a triangular wave voltage (5 V μm^{-1}, 10 Hz) for a representative compound **BC6-7** at 112 °C and two current response peaks were recorded during a half period of the applied field indicating antiferroelectric behaviour. The spontaneous polarization determined by integration of the switching current peaks amounts to 484 nC cm^{-2}. Thus, the phase under discussion is unambiguously SmCP$_A$.

Optical textural observations clearly showed the occurrence of two mesophases for compounds **BC6-16** and **BC6-18**. On cooling the isotropic liquid, the high temperature phase grows as bâtonnets that coalesce to form a focal-conic texture (Fig. 13a). Additionally, in a different region of the slide, a dark field of view was also seen, indicating the presence of a SmA phase. On further cooling, at the transition to the low temperature phase, on the focal-conic texture of the SmA phase some striations appear (Fig. 13b) whereas the homeotropic SmA regions fill with the schlieren texture. The X-ray diffraction study ensured the layered structure of the SmA phase of **BC6-18**: it showed a sharp reflection in the small angle region at d = 52.7 Å. The wide-angle diffuse peak at 4.6 Å indicates a liquid-like ordering of the molecules in the mesophase. Similarly, an X-ray profile obtained for the low temperature phase of **BC6-18** showed a strong Bragg reflection (60 Å) and its higher order reflection (29.3 Å) in the small angle region, indicating a layer structure. Further, the diffuse wide angle scattering (4.5 Å) indicates a liquid-like order within the smectic layer. Two current response peaks obtained per half period on application of a triangular wave voltage confirmed an antiferroelectric switching characteristic of the mesophase with the saturated polarization being about 379 nC cm^{-2}. Based on these results we have identified this mesophase as the SmCP$_A$ phase. It may be mentioned here that the SmA phase did not show any response to the applied electrical field.

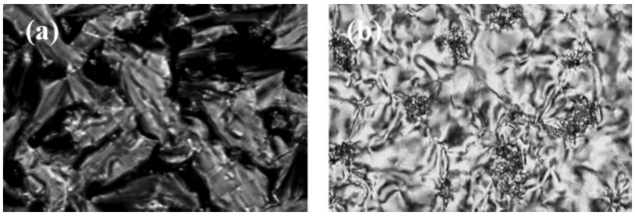

Fig. 12 Optical photomicrographs showing the broken fan-shaped (a) and schlieren (b) textures obtained in different regions for the SmCP phase of compound **BC6-7**.

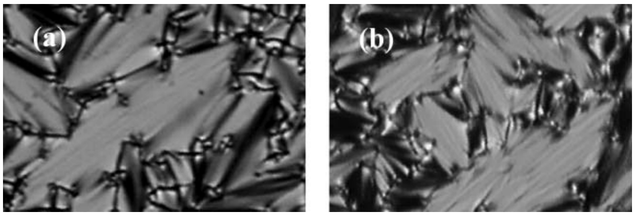

Fig. 13 Optical photomicrographs showing (a) focal-conic texture of SmA and (b) broken focal conics pattern of SmCP mesophases at 120 °C and 110 °C respectively, obtained for the compound **BC6-18**.

It can be seen that the melting temperatures of these 4-nitro derivatives are slightly lower than those of analogous non-substituted compounds and thereby exhibit a higher mesophase range. The relatively high values of the spontaneous polarization found in these homologues can be attributed to the enhancement of the lateral dipole moment by the polar nitro group. The transition from the SmCP phase to the conventional SmA phase in higher homologues obviously indicates that the bulky NO_2 substituent at the 4 position of the central 1,3-phenylene ring modifies the mesomorphic behaviour by exerting its influence on the bending angle between the two arms. Stabilization of different banana mesophases with different structural and electrical switching properties in structurally isomeric nitro-substituted derivatives (with substitutions at the 2 and 4 positions) clearly demonstrates the dependence of mesomorphic behaviour on the subtle changes in the molecular structures.

Summary

We have reported the synthesis and characterization of more than fifty novel banana-shaped compounds belonging to six different homologous series, the novelty of which originates from the fact that the molecular design comprises laterally substituted 1,3-phenylene ring as a central unit covalently linked to thermally and hydrolytically stable rod-like salicylaldimine segments (arms). It is well demonstrated that the nature (electro-negativity or polarizability and size) and position of these substituents generally decide the type of mesophase(s) and phase sequence to be formed by the banana-shaped compounds in which they are present. All the mesogens derived from 2-methylresorcinol exhibit an antiferroelectric SmCP phase with the exception of a higher homologue that displays an antiferroelectric B_X phase. In contrast to this, a methyl group present at the 5 position of the 1,3-phenylene ring reduces the clearing temperature as well as the thermal range of the antiferroelectric SmCP phase. Further, unlike in the case of the parent series of non-substituted analogues, banana-shaped compounds derived from 2- or 5-methylresorcinol suppress the formation of the B_7 phase irrespective of the lengths of the terminal alkoxy chains. The chlorine atom substituent near the linking groups, *i.e.* at the 4 and/or 6 position of the central 1,3-phenylene ring, is found to change the bending angle between the two arms and hence the mesomorphic behavior of the molecules, an observation in agreement with the literature reports. In general, mesogens derived form 4-chlororesorcinol exhibit an antiferroelectric SmCP phase. Compounds having short or long chain lengths (with one exception) display dimesomorphic SmCP–N and SmCP–SmC sequences respectively, whereas the middle homologues exhibit only the SmCP phase. Interestingly, a homologue with a docosanoxy tail displays a trimesomorphic SmCP–SmC–SmA sequence. Observation of the SmCP phase, characteristic for a bent molecular shape, and conventional phases like N, SmC and/or SmA occurring in the same substance suggest that in the context of molecular structures, the boundary between rod-like and banana-shaped mesogens is narrow and can be altered by having appropriate lateral substitutions at the central core. The 4,6-dichlororesorcinol derivatives exhibit only the N and/or SmC phases, supporting the view that the optimum bending angle required for the occurrence of banana mesophases is in the range of 110–140°. Compounds with 2-nitro substitution exclusively form a B_7 (non-switchable) phase irrespective of the terminal alkyl chain length they possess, in contrast to the antiferroelectric B_7 phase observed for non-substituted and methyl group containing analogues. On the other hand the thermal behavior of bent-core molecules derived from 4-nitroresorcinol was found to be different from the 2-nitro derivatives. The lower and middle homologues display an antiferroelectric SmCP phase whereas the higher ones exhibit the SmA phase additionally. The trend observed for the clearing temperatures in these homologues is unusual. For a particular homologous series of compounds with increasing number of carbon atoms in the chain, the transition temperatures can increase or decrease drastically or remain nearly the same. The SmCP phase stabilized by different homologues exhibit antiferroelectric switching behavior. Relatively high values of the spontaneous polarization, *i.e.* about 380–400 nC cm^{-2}, were found in the SmCP phases formed by 4-nitro derivatives. The B_7 phase observed for the bent-core molecules derived from 2-methylresorcinol derivatives show an antiferroelectric switching behavior though no such feature was observed for the B_7 phase formed by the 2-nitro derivatives. This points to the complex structural behavior of this phase and more investigations are needed to understand the properties of this phase. Thus, understanding the relationship between molecular architecture and liquid crystal properties in banana-shaped molecules is not straightforward, a feature often emphasized in the literature.

References

1 For elaborative reports on bent-core molecules see: (*a*) G. Pelzl, S. Diele and W. Weissflog, *Adv. Mater.*, 1999, **11**, 707; (*b*) C. Tschierske, *Annu. Rep. Prog. Chem., Sect. C*, 2001, **97**, 191; (*c*) C. Tschierske and G. Dantlgraber, *Pramana*, 2003, **61**, 455; (*d*) M. B. Ros, J. L. Serrano, M. R. de la Fuente and C. L. Folcia, *J. Mater. Chem.*, 2005, **15**, 5093; (*e*) R. Amaranatha Reddy and C. Tschierske, *J. Mater. Chem.*, 2006, **16**, 907; (*f*) H. Takezoe and Y. Takanishi, *Jpn. J. Appl. Phys.*, 2006, **45**, 597.

2 (*a*) D. Vorlander, *Ber. Dtsch. Chem. Ges.*, 1929, **62**, 2831; (*b*) D. Vorlander and A. Apel, *Ber. Dtsch. Chem. Ges.*, 1932, **65**, 1101.

3 T. Niori, T. Sekine, J. Watanabe, T. Furukawa and H. Takezoe., *J. Mater. Chem.*, 1996, **6**, 1231.

4 (*a*) M. Kuboshita, Y. Matsunaga and H. Matsuzaki, *Mol. Cryst. Liq. Cryst.*, 1991, **199**, 319; (*b*) T. Matsuda and Y. Matsunga, *Bull. Chem. Soc. Jpn.*, 1991, **64**, 2192; (*c*) H. Matsuzaki and Y. Matsunaga, *Liq. Cryst.*, 1993, **14**, 105; (*d*) T. Akutagawa, Y. Matsunaga and K. Yasuhara, *Liq. Cryst.*, 1994, **17**, 659; (*e*) Y. Matsunaga and S. Miyamoto, *Mol. Cryst. Liq. Cryst.*, 1993, **237**, 311.

5 G. Heppke, D. D. Parghi and H. Sawade., *Liq. Cryst.*, 2000, **27**, 313.

6 D. R. Link, G. Natale, R. Shao, J. E. Maclennan, N. A. Clark, E. Karblova and D. M. Walba., *Science*, 1997, **278**, 1924.

7 (*a*) The symbols B_1–B_7 to designate the banana phases were proposed in a workshop on banana-shaped liquid crystals, December 1997, Berlin, Germany; (*b*) S. Diele, G. Pelzl and W. Weisflog, *Liq. Cryst. Today*, 1999, **9**, 8.

8 H. R. Brand, P. E. Cladis and H. Pleiner, *Eur. Phys. J. B*, 1998, **6**, 347.

9 (*a*) R. Amaranatha Reddy, V. A. Raghunathan and B. K. Sadashiva, *Chem. Mater.*, 2005, **17**, 274 and references cited therein; (*b*) R. Amaranatha Reddy, B. K. Sadashiva and V. A. Raghunathan, *Chem. Mater.*, 2004, **16**, 4050; (*c*)

R. Amaranatha Reddy and B. K. Sadashiva, *J. Mater. Chem.*, 2004, **14**, 1936; (*d*) R. Amaranatha Reddy, B. K. Sadashiva and S. Dhara, *Chem. Commun.*, 2001, 1972; (*e*) R. Amaranatha Reddy and B. K. Sadashiva, *Liq. Cryst.*, 2000, **27**, 1613.

10 (*a*) J. Matraszek, J. Mieczkowski, J. Szydlowska and E. Gorecka, *Liq. Cryst.*, 2000, **27**, 429; (*b*) J. Szydlowska, J. Mieczkowski, J. Matraszek, D. W. Bruce, E. Gorecka, D. Pociecha and D. Guillon, *Phys. Rev. E*, 2003, **67**, 031702; (*c*) U. Duneman, M. W. Schroeder, G. Pelzl, S. Diele and W. Weissflog, *Liq. Cryst.*, 2005, **32**, 151.

11 (*a*) V. Gortz and J. W. Goodby, *Chem. Commun.*, 2005, 3262; (*b*) L. A. Madsen, T. J. Dingemans, M. Nakata and E. T. Samulski, *Phys. Rev. Lett.*, 2004, **92**, 145505; (*c*) S. I. Torgova, T. A. Geivandova, O. Francescangeli and A. Strigazzi, *Pramana*, 2003, **61**, 239; (*d*) T. J. Dingemans and E. T. Samulski, *Liq. Cryst.*, 2000, **27**, 131.

12 (*a*) B.-K. So, Y.-S. Kim, M.-M. Choi, S.-M. Lee, J.-E. Kim, H. H. Song and J.-H. Park, *Liq. Cryst.*, 2004, **31**, 169; (*b*) R. Mahajan, H. Nandedkar and A. Vora, *Liq. Cryst.*, 2004, **31**, 585; (*c*) C. V. Yelamaggad, S. Anitha Nagamani, U. S. Hiremath, D. S. Shankar Rao and S. Krishna Prasad, *Liq. Cryst.*, 2002, **29**, 1401; (*d*) V. Prasad, D. S. Shankar Rao and S. Krishna Prasad, *Liq. Cryst.*, 2000, **27**, 585.

13 (*a*) P. Pyc, J. Mieczkowski, D. Pociecha, E. Gorecka, B. Donnio and D. Guillon, *J. Mater. Chem.*, 2004, **14**, 2374; (*b*) V. Prasad, S.-W. Kang, K. A. Suresh, L. Joshi, Q. Wang and S. Kumar, *J. Am. Chem. Soc.*, 2005, **127**, 17224; (*c*) H. T. Nguyen, J. P. Bedel, J. C. Marcerou and M. F. Achard, *Pramana*, 2003, **61**, 395; (*d*) V. Prasad, S.-W. Kang and S. Kumar, *J. Mater. Chem.*, 2003, **13**, 1259; (*e*) W. Weissflog, G. Naumann, B. Kosata, M. W. Schroeder, A. Eremin, S. Diele, Z. Vakhovskaya, H. Kresse, R. Friedemann, S. Ananda Rama Krishan and G. Pelzl, *J. Mater. Chem.*, 2005, **15**, 4328.

14 (*a*) W. Weissflog, H. Nadasi, U. Dunemann, G. Pelzl, S. Diele, A. Eremin and H. Kresse, *J. Mater. Chem.*, 2001, **11**, 2748; (*b*) U. Dunemann, M. W. Schroeder, R. Amaranatha Reddy, G. Pelzl, S. Diele and W. Weissflog, *J. Mater. Chem.*, 2005, **15**, 4051; (*c*) G. Pelzl, S. Diele, S. Grande, A. Jakli, C. Lischka, H. Kresse, H. Schmalfuss, I. Wirth and W. Weissflog, *Liq. Cryst.*, 1999, **26**, 401; (*d*) W. Weissflog, C. Lischka, S. Diele, G. Pelzl and I. Wirth, *Mol. Cryst. Liq. Cryst.*, 1999, **328**, 101; (*e*) W. Weissflog, C. Lischka, S. Diele, G. Pelzl, I. Wirth, S. Grande, H. Kresse, H. Schmalfuss, H. Hartung and A. Stettler, *Mol. Cryst. Liq. Cryst.*, 1999, **333**, 203; (*f*) S. Diele, S. Grande, H. Kruth, C. Lischka, G. Pelzl, W. Weissflog and I. Wirth, *Ferroelectrics*, 1998, **212**, 169; (*g*) G. Pelzl, S. Diele, A. Jakli, C. Lischka, I. Wirth and W. Weissflog, *Liq. Cryst.*, 1999, **26**, 135; (*h*) W. Weissflog, L. Kovalenko, I. Wirth, S. Diele, G. Pelzl, H. Schmalfuss and H. Kresse., *Liq. Cryst.*, 2000, **27**, 677; (*i*) W. Weissflog, C. Lischka, T. Benne, T. Scharf, G. Pelzl, S. Diele and H. Kruth, *Proc. SPIE—Int. Soc. Opt. Eng.*, 1998, **3319**, 14; (*j*) I. Wirth, S. Diele, A. Eremin, G. Pelzl, S. Grande, L. Kovalenko, N. Pancenko and W. Weissflog, *J. Mater. Chem.*, 2001, **11**, 1642.

15 (*a*) J. Mieczkowski, J. Szydlowska, J. Matraszek, D. Pociecha, E. Gorecka, B. Donnio and D. Guillon, *J. Mater. Chem.*, 2002, **12**, 3392; (*b*) M. Kaspar, V. Hamplova, V. Novotna, M. Glogarova and P. Vanek, *J. Mater. Chem.*, 2002, **12**, 2221.

16 (*a*) S. Umadevi, S. Radhika and B. K. Sadashiva, *Liq. Cryst.*, 2006, **33**, 139; (*b*) R. Amaranatha Reddy and B. K. Sadashiva, *Liq. Cryst.*, 2003, **30**, 1031; (*c*) H. N. Shreenivasa Murthy and B. K. Sadashiva, *Liq. Cryst.*, 2002, **29**, 1223; (*d*) B. K. Sadashiva, H. N. Shreenivasa Murthy and D. Surajit, *Liq. Cryst.*, 2001, **28**, 483; (*e*) R. Amaranatha Reddy and B. K. Sadashiva, *Liq. Cryst.*, 2004, **31**, 1069.

17 J. P. Bedel, J. C. Rouillon, J. P. Marcerou, M. Laguerre, H. T. Nguyen and M. F. Achard, *Liq. Cryst.*, 2000, **27**, 1411.

18 K. W. Wang, A. Jakli, H. Li, Y. Yang and J. Wen, *Liq. Cryst.*, 2001, **28**, 1705 and references cited therein.

19 (*a*) E. Gorecka, D. Pociecha, J. Mieczkowski, J. Matraszek, D. Guillon and B. Donnio, *J. Am. Chem. Soc.*, 2004, **126**, 15946; (*b*) D. M. Walba, E. Korblova, R. Shao, J. E. Maclennan, D. R. Lonk, M. A. Glaser and N. A. Clark, *Science*, 2000, **288**, 2181; (*c*) G. Heppke, D. D. Parghi and H. Sawade., *Mol. Cryst. Liq. Cryst.*, 2000, **352**, 311.

20 (*a*) G. Dantlgraber, A. Eremin, S. Diele, A. Hauser, H. Kresse, G. Pelzl and C. Tschierske, *Angew. Chem., Int. Ed.*, 2002, **41**, 2408; (*b*) C. Keith, R. Amaranatha Reddy, H. Hahn, H. Lang and C. Tschierske, *Chem. Commun.*, 2004, 1898.

21 D. Kardas, M. Prehm, U. Baumeister, D. Pociecha, R. Amaranatha Reddy, G. H. Mehl and C. Tschierske, *J. Mater. Chem.*, 2005, **15**, 1722.

22 (*a*) C. V. Yelamaggad, U. S. Hiremath, S. A. Nagamani, D. S. Shankar Rao and S. K. Prasad, *J. Mater. Chem.*, 2001, **11**, 1818; (*b*) D. S. Shankar Rao, Geetha G. Nair, S. Krishna Prasad, S. Anitha Nagamani and C. V. Yelamaggad, *Liq. Cryst.*, 2001, **28**, 1239; (*c*) S. K. Prasad, Y. Maeda, D. S. Shankar Rao, S. A. Nagamani, U. S. Hiremath and C. V. Yelamaggad, *Liq. Cryst.*, 2003, **30**, 1277; (*d*) C. V. Yelamaggad, S. A. Nagamani, G. G. Nair, D. S. Shankar Rao, S. K. Prasad and A. Jakli, *Liq. Cryst.*, 2002, **2**, 1181.

23 D. M. Walba, E. Korblova, R. Shao and N. A. Clark, *J. Mater. Chem.*, 2001, **11**, 2743.

24 R. Achten, A. Koudijs, Z. Karczmarzyk, A. T. M. Marcelis and E. J. R. Sudholter, *Liq. Cryst.*, 2004, **31**, 215.

25 (*a*) H. N. Shreenivasa Murthy and B. K. Sadashiva, *J. Mater. Chem.*, 2003, **13**, 2863; (*b*) H. N. Shreenivasa Murthy and B. K. Sadashiva, *Liq. Cryst.*, 2003, **30**, 1051; (*c*) R. Amaranatha Reddy and B. K. Sadashiva, *Liq. Cryst.*, 2003, **30**, 273; (*d*) R. Amaranatha Reddy and B. K. Sadashiva, *Liq. Cryst.*, 2002, **29**, 1365.

26 W. Weissflog, H. N. Shreenivasa Murthy, S. Diele and G. Pelzl, *Philos. Trans. R. Soc. London, Ser. A*, 2006, **364**, 2657.

27 K. Fodor-Csorba, A. Vajda, A. Jakli, C. Slugovc, G. Trimmel, D. Demus, E. Gacs-Baitz, S. Holly and G. Galli, *J. Mater. Chem.*, 2004, **14**, 2499.

28 S. Umadevi and B. K. Sadashiva, *Liq. Cryst.*, 2005, **32**, 1233.

29 G. Pelzl, H. N. Shreenivasa Murthy, M. W. Schröder, S. Diele, Z. Vakhovskaya, H. Kresse and W. Weissflog, *J. Mater. Chem.*, 2006, **16**, 1702.

30 W. Weissflog, M. W. Schröder, S. Diele and G. Pelzl, *Adv. Mater.*, 2003, **15**, 630.

31 L. Kovalenko, W. Weissflog, S. Grande, S. Diele, G. Pelzl and I. Wirth, *Liq. Cryst.*, 2000, **27**, 683.

32 H. N. Shreenivasa Murthy, M. Bodyagin, S. Diele, U. Baumeister, G. Pelzl and W. Weissflog, *J. Mater. Chem.*, 2006, **16**, 1634.

33 W. Weissflog, S. Sokolowski, H. Dehne, Banani Das, S. Grande, M. W. Schröder, A. Eremin, S. Diele, G. Pelzl and H. Kresse, *Liq. Cryst.*, 2004, **31**, 923.

34 L. Kovalenko, M. W. Schröder, R. Amaranatha Reddy, S. Diele, G. Pelzl and W. Weissflog, *Liq. Cryst.*, 2005, **32**, 857.